The Duplicated B-Class Heterodimer Model: Whorl-Specific Effects and Complex Genetic Interactions in *Petunia hybrida* Flower Development

Michiel Vandenbussche,[a] Jan Zethof,[a] Stefan Royaert,[b] Koen Weterings,[b] and Tom Gerats[a,1,2]

[a] Department of Plant Systems Biology, Vlaams Instituut voor Biotechnologie/Ghent University, B-9052 Zwijnaarde, Belgium
[b] Department of Experimental Botany, Plant Genetics, University of Nijmegen, 6525ED Nijmegen, The Netherlands

In both Antirrhinum (*Antirrhinum majus*) and Arabidopsis (*Arabidopsis thaliana*), the floral B-function, which specifies petal and stamen development, is embedded in a heterodimer consisting of one DEFICIENS (DEF)/APETALA3 (AP3)-like and one GLOBOSA (GLO)/PISTILLATA (PI)-like MADS box protein. Here, we demonstrate that gene duplications in both the *DEF/AP3* and *GLO/PI* lineages in *Petunia hybrida* (petunia) have led to a functional diversification of their respective members, which is reflected by partner specificity and whorl-specific functions among these proteins. Previously, it has been shown that mutations in *PhDEF* (formerly known as *GREEN PETALS*) only affect petal development. We have isolated insertion alleles for *PhGLO1* (*FLORAL BINDING PROTEIN1*) and *PhGLO2* (*PETUNIA MADS BOX GENE2*) and demonstrate unique and redundant properties of *PhDEF*, *PhGLO1*, and *PhGLO2*. Besides a full homeotic conversion of petals to sepals and of stamens to carpels as observed in *phglo1 phglo2* and *phdef phglo2* flowers, we found that gene dosage effects for several mutant combinations cause qualitative and quantitative changes in whorl 2 and 3 meristem fate, and we show that the PHDEF/PHGLO1 heterodimer controls the fusion of the stamen filaments with the petal tube. Nevertheless, when the activity of *PhDEF*, *PhGLO1*, and *PhGLO2* are considered jointly, they basically appear to function as *DEF/GLO* does in Antirrhinum and to a lesser extent as *AP3/PI* in Arabidopsis. By contrast, our data suggest that the function of the fourth B-class MADS box member, the paleo*AP3*-type *PETUNIA HYBRIDA TM6* (*PhTM6*) gene, differs significantly from the known eu*AP3*-type DEF/AP3-like proteins; *PhTM6* is mainly expressed in the developing stamens and ovary of wild-type flowers, whereas its expression level is upregulated in whorls 1 and 2 of an A-function floral mutant; *PhTM6* is most likely not involved in petal development. The latter is consistent with the hypothesis that the evolutionary origin of the higher eudicot petal structure coincided with the appearance of the eu*AP3*-type MADS box genes.

INTRODUCTION

In the classical ABC model for flower development (Coen and Meyerowitz, 1991), the B-function in combination with the A-function was proposed to specify the development of petals in the second whorl and, together with the C-function, the development of stamens in the third whorl. In Arabidopsis (*Arabidopsis thaliana*) and *Antirrhinum majus* (snapdragon), the B-function is encoded by a pair of MADS box genes (*DEFICIENS* [*DEF*] and *GLOBOSA* [*GLO*] in *A. majus* and *APETALA3* [*AP3*] and *PISTILLATA* [*PI*] in Arabidopsis), and mutations in either one of these genes cause homeotic conversions of petals into sepals and stamens into carpels (Bowman et al., 1989; Sommer et al., 1990; Trobner et al., 1992; Goto and Meyerowitz, 1994; Jack

et al., 1994). Consistent with their crucial role in petal and stamen development, B-class genes are predominantly expressed in second- and third-whorl floral organ primordia, and their expression is maintained until petals and stamens have fully developed. *DEF* and *AP3* on the one hand and *GLO* and *PI* on the other hand belong to distinct but closely related MADS box subfamilies, referred to as the *DEF/AP3* and *GLO/PI* subfamilies (Purugganan et al., 1995; Theissen et al., 1996) and together as the B-class MADS box genes. Further, it has been shown with a variety of approaches that DEF and GLO in *A. majus* (Trobner et al., 1992) as AP3 and PI in Arabidopsis (Goto and Meyerowitz, 1994; Jack et al., 1994; Krizek and Meyerowitz, 1996; McGonigle et al., 1996; Riechmann et al., 1996; Yang et al., 2003a, 2003b) act jointly as a heterodimer and that in both species, the initially low expression level of both genes is enhanced and maintained by feedback stimulation through the heterodimeric protein complex itself. Because the B-class genes analyzed in Arabidopsis and *A. majus* appeared to be highly similar in number and function, it was initially proposed that the function and mode of action of *DEF/AP3* and *GLO/PI* homologs as B-class organ identity genes would be exemplary for eudicot species. However, data are accumulating suggesting that B-function regulation varies within the eudicot lineage. Expression studies of B-class MADS box genes in several lower eudicot species

revealed that their expression patterns during petal development differ significantly from those observed in Arabidopsis and *A. majus*, although they are comparable during stamen development (Kramer and Irish, 1999). In addition, several of these basal angiosperm B-class MADS box genes are also expressed in carpels and developing ovules (Kramer and Irish, 1999, 2000; Kramer et al., 2003). In many plant species, more than one *DEF/AP3* and/or *GLO/PI* family member has been isolated, indicating that the B-class lineages have been subjected to duplications and subsequent functional divergence during evolution. More specifically, a major duplication event in the *DEF/AP3* subfamily coincides with the origin of the higher eudicot radiation (Kramer et al., 1998). The resulting two types of DEF/AP3-like proteins can easily be distinguished on the basis of their completely divergent C-terminal motifs, which have been named the paleo*AP3* and eu*AP3* motifs. Interestingly, the eu*AP3* motif is exclusively found in DEF/AP3 proteins isolated from higher eudicots, whereas the paleo*AP3* motif is encountered in DEF/AP3 proteins throughout the lower eudicots, magnoliid dicots, monocots, and basal angiosperms. In addition, a number of higher eudicot species contain both the eu*AP3* and paleo*AP3* type of genes, termed eu*AP3* and *TOMATO MADS BOX GENE6* (*TM6*) lineages, respectively (Kramer and Irish, 2000). Recently, we have shown that the eu*AP3* motif most likely resulted from a simple frameshift mutation in one of the copies of a duplicated ancestral paleo*AP3*-type gene (Vandenbussche et al., 2003a), and data were published indicating that paleo*AP3* and eu*AP3* motifs encode divergent functions (Lamb and Irish, 2003), supporting the hypothesis that eu*AP3* genes may have acquired a novel function compared with paleo*AP3* genes, most likely in petal development (Kramer et al., 1998).

All data together suggest that considerable variations in B-function regulation exist among the eudicots. To investigate this further, we have initiated a functional analysis of the *Petunia hybrida* (petunia) B-class MADS box genes. *P. hybrida* is a good model system to study the effects of gene duplication and functional divergence within the B-class MADS box gene lineages because four B-class MADS box genes have been identified in *P. hybrida*, of which *PhGLO1* (*FLORAL BINDING PROTEIN1* [*FBP1*]) and *PhGLO2* (*PETUNIA MADS BOX GENE2* [*PMADS2*]) belong to the *GLO/PI* subfamily, whereas *PhDEF* (*GREEN PETALS* [*GP*]) and *PETUNIA HYBRIDA TM6* (*PhTM6*) within the *DEF/AP3* subfamily belong to the eu*AP3* and paleo*AP3* lineages (*TM6* lineage), respectively (Angenent et al., 1992, 1993; van der Krol et al., 1993; Kramer and Irish, 2000). It has been demonstrated before that mutations in *PhDEF* (*GP*) cause homeotic transformations in only one whorl. In this mutant, petals are converted to sepals, whereas stamens remain virtually unaffected (de Vlaming et al., 1984; van der Krol et al., 1993). In addition, it was shown that the expression levels of *PhGLO1* and *PhGLO2* were reduced in the second whorl of *phdef* flowers but not in the stamens, suggesting that B-function regulation differs between the second and third whorls in *P. hybrida* flowers (van der Krol et al., 1993). The function of *PhGLO1* was analyzed previously using a cosuppression approach (Angenent et al., 1993), but our results indicate that downregulation in these lines did not occur in a gene-specific way (cf. Vandenbussche et al., 2003b). Interestingly, although *PhGLO1* is highly expressed

throughout stamen development, the PHGLO1 protein was immunologically not detectable in these organs later in development, suggesting a posttranscriptional regulation of PhGLO1 expression in later stages of stamen development (Caňas et al., 1994). In a general screening for insertions into any member of the *P. hybrida* MADS box gene family, we have identified transposon insertion mutants for the two *P. hybrida GLO/PI* homologs (Vandenbussche et al., 2003b). Here, we present a functional characterization of the *P. hybrida* B-class MADS box genes by a combination of single and double mutant analyses, two-hybrid interaction studies, and a detailed expression analysis of the four B-class MADS box genes in wild-type and various mutant backgrounds. Based on these results, we propose a model describing unique and overlapping functions of the different putative B-class heterodimers in *P. hybrida*, and we discuss similarities and differences in B-function regulation between the three eudicot species *P. hybrida*, Antirrhinum, and Arabidopsis.

RESULTS

Phylogenetic Analysis

The phylogenetic relationship between the *P. hybrida*, Antirrhinum, and Arabidopsis B-class MADS box genes is represented
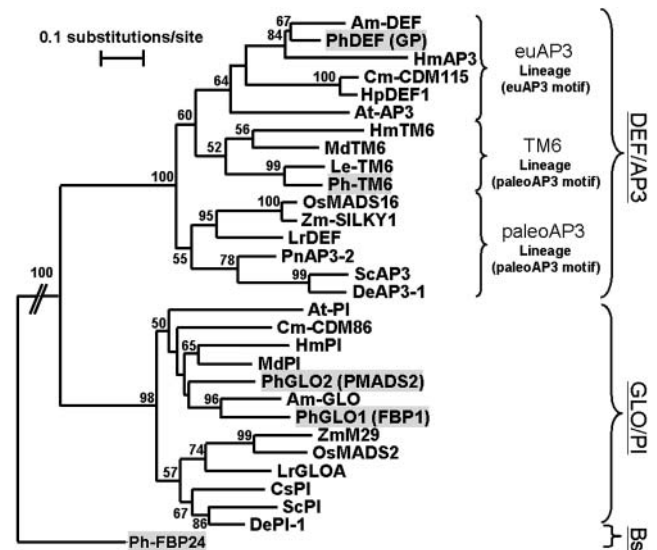

Figure 1. Neighbor-Joining Tree of B-Class MADS Box Genes from *P. hybrida*, Arabidopsis, *A. majus*, and a Selection of Other Species.

Species names are indicated as follows: Am, *A. majus*; At, *A. thaliana*; Cm, *Chrysanthemum x morifolium*; Cs, *Chloranthus spicatus*; De, *Dicentra eximia*; Hp, *Hieracium piloselloides*; Hm, *Hydrangea macrophylla*; Md, *Malus x domestica*; Le, *L. esculentum*; Lr, *Lilium regale*; Os, *O. sativa*; Ph, *P. hybrida* (shaded); Pn, *Papaver nudicaule*; Sc, *Sanguinaria canadensis*; and Zm, *Z. mays*. We renamed three of the four *P. hybrida* putative B-function proteins; old names are shown in between brackets. The tree was rooted with FBP24, a *P. hybrida* member of the B$_{sister}$ (B$_s$) MADS box subfamily (Becker et al., 2000). Altogether, 1000 bootstrap samples were generated to assess support for the inferred relationships. Local bootstrap probabilities (in percentages) are indicated near the branching points.

by a neighbor-joining tree (Figure 1), which was constructed by comparing the MIK domain of these sequences, including a selection of sequences from other taxonomic groups. The *FBP24* gene, a *P. hybrida* member of the B$_{sister}$ subfamily (Becker et al., 2002), was used as an outgroup. For a more comprehensive overview of B-class MADS box genes, we refer to Kramer et al. (1998), Kramer and Irish (2000), and Vandenbussche et al. (2003a). The phylogenetic analysis indicates that in *P. hybrida*, gene duplications have occurred in both the *GLO/PI* and *DEF/AP3* lineages. To facilitate mental comparisons between the different systems, we have decided to rename the *GP*, *FBP1*, and *PMADS2* genes to *PhDEF*, *PhGLO1*, and *PhGLO2*, respectively, after the founding members of the different subfamilies; *PhTM6* was previously named after *TM6*, the *Lycopersicon esculentum* (tomato) paleo*AP3* representative (Kramer and Irish, 2000). *PhGLO1* and *PhGLO2* are more closely related to *GLO* than to *PI*, which is in accordance with the taxonomic distribution of the species involved; *P. hybrida* and *A. majus* belong to the Asteridae, whereas Arabidopsis belongs to the Rosidae. Likewise, *PhDEF* displays a closer phylogenetic relationship to *DEF* than to *AP3*, whereas the second *P. hybrida DEF/AP3* member, *PhTM6*, belongs to the so-called *TM6* lineage, which forms a distinct clade within the *DEF/AP3* subfamily (Kramer and Irish, 2000).

Analysis of *phglo1* and *phglo2* Single Mutants

To further characterize the B-function in *P. hybrida*, we have screened for transposon insertions into the *PhGLO1*, *PhGLO2*, and *PhTM6* genes; *phdef* alleles were already available (de Vlaming et al., 1984; van der Krol et al., 1993). In this screening, we identified transposon insertions in two of our three primary targets, *PhGLO1* and *PhGLO2*. The *phglo1-1* and *phglo1-2* alleles (Table 1) were isolated in a forward genetics manner (Van den Broeck et al., 1998; Vandenbussche et al., 2003b; M. Sauer, unpublished data) and contain a *dTph1* insertion in the C-terminal domain and a *dTph8* insertion in the K region, respectively. Flowers of plants homozygous for the *phglo1-1* or *phglo1-2* allele display an identical phenotype: the midveins of the petals become broader and greener, especially toward the edge of the corolla at the abaxial side of the petals (Figures 2A and 2B).

Scanning electron microscopy of these regions revealed a conversion of the typical conical petal epidermal cells into sepal-like epidermal cells, the presence of stomata, and the development of trichomes, suggesting a shift of petal toward sepal identity in these regions (Figures 2C to 2E). In wild-type *P. hybrida* flowers, stamen filaments are fused partly with the corolla tube. By contrast, stamen filaments of *phglo1* mutants are not fused (Figure 2F). Mutants for *PhGLO1* thus exhibit a very partial B-mutant phenotype.

The *phglo2-1, phglo2-2*, and *phglo2-3* insertion alleles (Table 1) were identified in a reverse genetics screening (Vandenbussche et al., 2003b). Flowers of plants homozygous for any of these three insertion alleles appear morphologically as wild type (data not shown). However, we occasionally observed flowers of homozygous mutants with anthers that failed to dehisce properly. These anthers shrivel and become brownish at the time mature pollen grains are released from wild-type anthers. Because of the low penetration of the phenotype, we have not analyzed this phenomenon in detail.

To further elucidate the genetic interactions among these genes, we have selected all possible double mutant combinations using the available mutant alleles (Table 1).

phglo1 phglo2 Double Mutant Analysis

Besides plants displaying a wild-type or a *phglo1* phenotype, three new phenotypic classes were encountered in the F2 progeny of the *phglo1* × *phglo2* cross. A first class consisted of plants that exhibit a complete conversion of petals to sepals and of stamens to carpels (Figure 2G). The five carpelloid organs in the third whorl are fused and form a central tubular structure. Development of the genuine bilocular gynoecium formed in the fourth whorl of the wild-type flower often is strongly reduced. Molecular analysis indicated these plants to be the expected homozygous double mutants. Because *phglo1* and *phglo2* single mutants both develop petals and stamens, this indicates that at least one of the two *GLO/PI* genes must be active to enable B-function activity in the flower. In a second class, an unexpected phenotype was encountered: plants exhibiting a qualitative change of anthers into carpels, whereas petal identity remained

Table 1. Description of Identified *P. hybrida* B-Class MADS Box Gene Mutant Alleles and New Nomenclature

Subfamily	Subfamily Members	Mutant Allele	Mutagen	Insertion Position (ATG Start Codon = 1) 5′ of ATG	In the ORF	Ref.	New Gene Names + Corresponding Alleles
DEF/AP3	*GP*	*gp (R100)*	EMS	NA		1	*PHDEF* **phdef-1**
		gp (PLV)	γ-Radiation	Chromosomal deletion		2	phdef-2
GLO/PI	*FBP1*	*fbp1-1*	*dTph1*		+599 bp	3	*PHGLO1* phglo1-1
		fbp1-2	*dTph8*		+411 bp	4	**phglo1-2**
	PMADS2	*pmads2-1*	*dTph1*	−171 bp		4	*PHGLO2* phglo2-1
		pmads2-2	*dTph1*	−84 bp		4	phglo2-2
		pmads2-3	*dTph1*		+49 bp	4	**phglo2-3**

Insertion alleles selected for further crosses in bold. NA, not applicable.
Ref. 1, de Vlaming et al. (1984); Ref. 2, van der Krol et al. (1993); Ref. 3, Van den Broeck et al. (1998), M. Sauer, unpublished data; Ref. 4, Vandenbussche et al. (2003b).
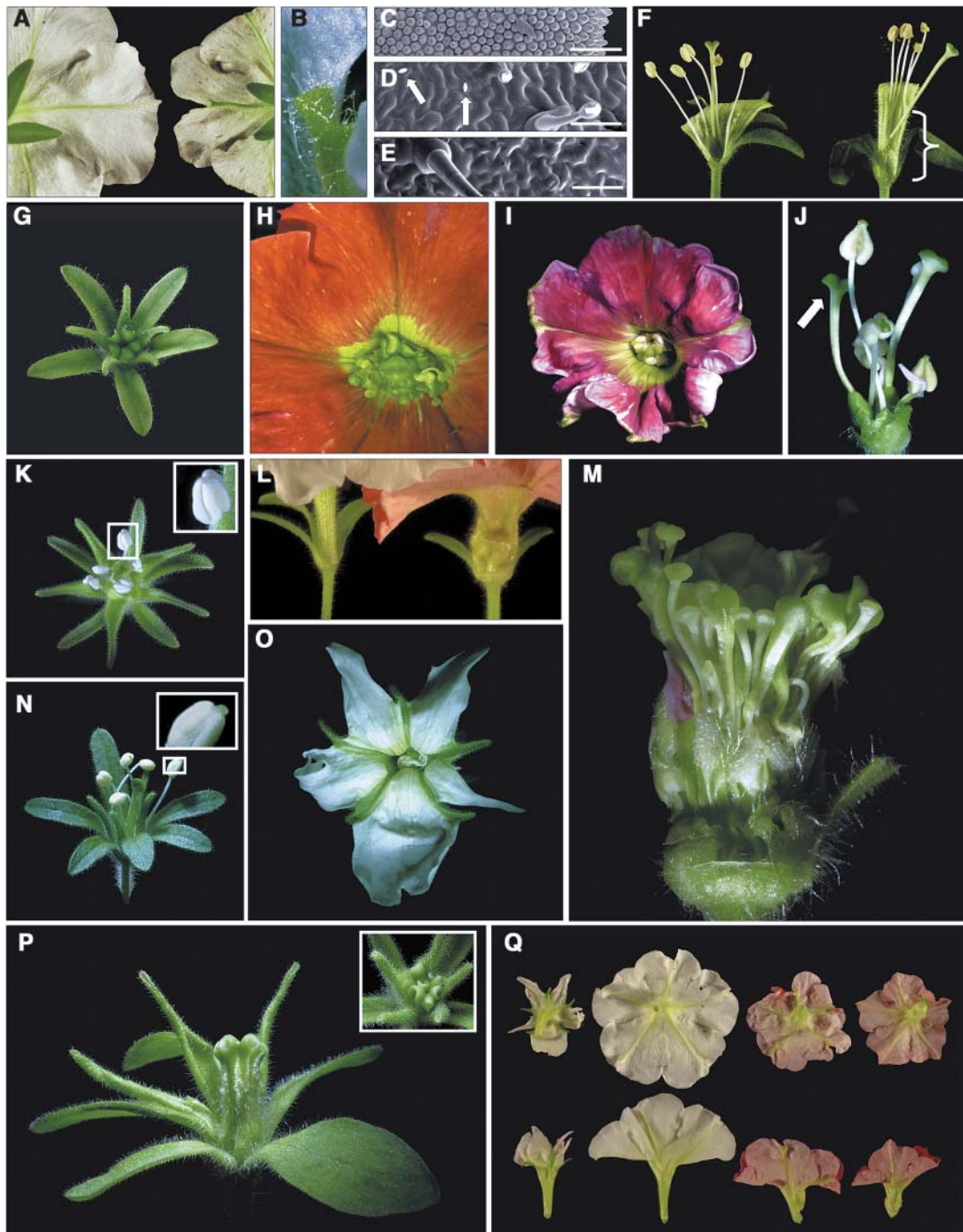
Figure 2. Phenotypes Observed in *phglo1* Flowers and in the F2 Progenies of the *phglo1 phglo2*, *phdef phglo1*, and *phdef phglo2* Crosses.

(A) to **(F)** Phenotypic analysis of *phglo1-2* mutants.
(A) Abaxial side of wild-type (left) and *phglo1-2* (right) petals.
(B) Close-up of a *phglo1-2* petal showing green tissue and trichomes.
(C) to **(E)** Scanning electron microscopy images of the adaxial epidermis of wild-type petals **(C)** showing the characteristic conical petal cells; *phglo1-2* petals **(D)** near a midvein at the edge of the corolla showing sepal-like epidermal cells, trichomes and stomata (arrows); and wild-type sepal **(E)** with typical sepal epidermis cells, trichomes, and stomata. Scale bars = 100 μm for **(C)** to **(E)**.
(F) *phglo1-2* flower (left) with freestanding stamen filaments and wild-type flower (right) with part of the stamen filaments fused to the corolla tube (indicated by a white brace); corolla and sepals have been removed partially to reveal the inner organs.

largely unaffected (Figure 2H). Moreover, the base of the petal tube in these flowers was considerably enlarged, and petal tube length and size of the corolla were reduced compared with wild-type and *phglo1* single mutant flowers (Figures 2L and 2Q). Furthermore, there is a strong increase in third-whorl organ number, mainly consisting of numerous carpelloid structures, although rudimentary petaloid structures develop regularly in between these organs and the second-whorl petals. Often, ovules and placental tissue develop on and in between these third-whorl organs without being encapsulated in an ovary (Figure 2M). In contrast with *phglo1 phglo2* double mutants, the wild-type bilocular gynoecium develops normally in plants of this class, although it can be partially fused with carpelloid tissue from the third whorl (Figure 2H). All analyzed plants belonging to this class turned out to be homozygous mutant for *phglo2* and heterozygous for *phglo1*. A third class consisted of plants displaying a more pronounced phenotype than the subtle *phglo1* single mutants (Figures 2I and 2Q). The partial conversion of petal to sepaloid tissue along the petal midveins is more outspoken, and in the majority of the flowers, stigmatic tissue develops on top of the anthers in the third whorl. Occasionally, a stamen was fully converted into a carpel (Figure 2J). Longitudinal growth of the petal tube and corolla is reduced compared with wild-type and single *phglo1* mutants (Figure 2Q). Genotype analyses revealed that all tested plants of this class were homozygous mutant for *phglo1* and heterozygous for *phglo2*. Remarkably, we thus found gene dosage effects for both the *PhGLO1phglo1 phglo2* and the *phglo1 PhGLO2phglo2* genotypes.

phdef phglo1 Double Mutant Analysis

Apart from plants displaying the *phdef* mutant phenotype (Figure 2K), the *phglo1* mutant phenotype (Figure 2A), or a wild-type phenotype, two additional phenotypic classes were observed in the F2 progeny. First, we noticed plants that look very similar to *phdef* single mutants, except that they systematically develop stigmatoid tissue on top of the anthers (Figure 2N). Genotyping confirmed that these plants were *phdef phglo1* double mutants. The second group consisted of plants with flowers displaying a strongly enhanced *phglo1* phenotype, resulting in a particularly attractive new type of *P. hybrida* flower (Figures 2O and 2Q). The partial conversion of petals to sepals is more outspoken than in *phglo1* single mutants, especially along the petal midveins. The corolla tissue in between the enlarged green midveins displays full petal identity, although the total corolla surface is considerably reduced compared with *phglo1* single mutants. All of these plants appeared homozygous mutant for *phglo1* while heterozygous for *phdef*, again indicating the occurrence of gene dosage effects.

phdef phglo2 Double Mutant Analysis

In the F2 progeny of this cross, two phenotypes were encountered, besides wild type–appearing plants and plants with the *phdef* phenotype. One class consisted of plants with flowers exhibiting a complete conversion of petals to sepals and of anthers to carpels (Figure 2P). Genotyping revealed that these plants were *phdef phglo2* double mutants. The phenotype of these plants is strikingly similar to that of *phglo1 phglo2* double mutants, although in general, the carpelloid tubes of the latter were more regularly organized than in *phdef phglo2* mutants (cf. Figure 2G with 2P, inset). In both cases, the outer wall of the central carpelloid tube is densely covered with trichomes, which are never found in the inner two whorls of wild-type flowers, and development of the fourth-whorl pistil is often strongly reduced. These phenotypic effects are very similar to what has been observed in *def* and *glo* mutants in Antirrhinum (Sommer et al., 1990; Trobner et al., 1992). The phenotype of *phdef phglo2* flowers further clearly demonstrates that *PhDEF* is involved in anther development, which has remained elusive so far because *phdef* single mutants exhibit normal anthers. Plants of the second class (data not shown) displayed a phenotype similar to the

---

Figure 2. (continued).

(G) Flower of a *phglo1 phglo2* double mutant displaying full homeotic conversion of petals to sepals in the second whorl and of stamens to carpels in the third whorl, which are fused in a pentalocular gynoecium. Development of the central pistil is reduced.

(H) *PhGLO1phglo1 phglo2* flower showing second-whorl organs with normal petal identity, whereas stamens are converted to multiple carpelloid organs. Development of the central pistil appears as wild type.

(I) and **(J)** *phglo1 PhGLO2phglo2* flowers showing petals with a more pronounced petal to sepal conversion along the midveins compared with *phglo1* mutants **(I)**, stamens carrying stigmatic tissue on top of the anthers **(J)**, and one stamen that has been fully converted to a wild type–appearing pistil (indicated with an arrow). Sepals and petals have been removed to reveal the inner organs.

(K) Flower of a *phdef* mutant displaying full conversion of petals to sepals, whereas the anthers remain unaffected (inset).

(L) and **(M)** *PhGLO1phglo1 phglo2* flowers showing enlargement **(L)** of the petal tube base (right) compared with the wild type (left), sepals have been removed partially; third-whorl organs **(M)** consisting of multiple carpelloid organs and the presence of placental tissue carrying ovules without being encapsulated in an ovary. Extra petal tissue (red) is emerging between second- and third-whorl organs. First- and second-whorl organs have been removed.

(N) *phdef phglo1* flower with anthers carrying small stigmas on top (inset).

(O) Flower of a *PhDEFphdef phglo1* mutant with pronounced sepal-like petal midveins and asymmetrically reduced development of petal tissue in between.

(P) *phdef phglo2* flower displaying full conversion of petals to sepals and of stamens to carpels, which are fused in a central gynoecium. Two second-whorl sepals have been removed to show the central carpelloid structure densely covered with trichomes. Inset, top view of the central gynoecium.

(Q) Abaxial (top row) and side views (bottom row) of B-function gene mutant combinations, showing variations in corolla and tube structure. From left to right: *PhDEFphdef phglo1*, *phglo1*, *phglo1 PhGLO2phglo2*, and *PhGLO1phglo1 phglo2*.

one shown in Figure 2N: flowers that look like *phdef* single mutants, except that they frequently develop stigmatic tissue on top of the anthers. Such plants proved to be homozygous for *phdef* and heterozygous for *phglo2*.

phglo1 bl, *phglo2 bl*, and *phdef bl* Double Mutant Analysis

To test whether the second-whorl defects observed in *phglo1* and *phdef* flowers are independent from organ identity, we have crossed these mutants with the *P. hybrida* A-function mutant *blind* (*bl*) (Vallade et al., 1987). Because of ectopic expression of the C-function gene *PMADS3* in whorls 1 and 2 (Tsuchimoto et al., 1993; Kater et al., 1998), *bl* flowers display homeotic conversion of the corolla limb into antheroid structures in the second whorl (Figure 3C) and under certain conditions of mainly the tips of the sepals into carpelloid tissue in the first whorl.

We have shown that the *phglo1* mutation affects petal development only locally in the petal midveins at the edge of the corolla. A very similar local homeotic change occurs in *phglo1 bl* flowers: the second-whorl antheroid organs carry small style–stigma structures on top (Figures 2B and 3A), indicating an absence of B-function activity only in the distal ends of these organs. Therefore, we conclude that the subtle second-whorl phenotype of *phglo1* is independent from organ identity. As expected, *phglo2 bl* flowers are indistinguishable from those of *bl* single mutants (cf. Figures 3C and 3F) because *phglo2* single mutants do not exhibit homeotic conversions. By contrast, although *phdef* flowers display a full homeotic conversion of petals to sepals, the effect of the *phdef* mutation on the development of the second-whorl antheroid organs in *bl* flowers is much less severe (Figures 3D and 3E). Instead, these second-whorl organs resemble those of *phglo1 bl* (Figures 3A and 3B), exhibiting antheroid organs carrying small style–stigma structures on top. Furthermore, the tube often is replaced by five separate filamentous structures, whereas if present, the tube usually is more greenish, and its longitudinal outgrowth remains rather restricted (Figure 3E, inset). The same phenotype was obtained using another *phdef* allele (Table 1, *gp* [PLV]) crossed with the *bl* mutant (Tsuchimoto et al., 2000). These results are quite surprising because *phdef* single mutants have second-whorl
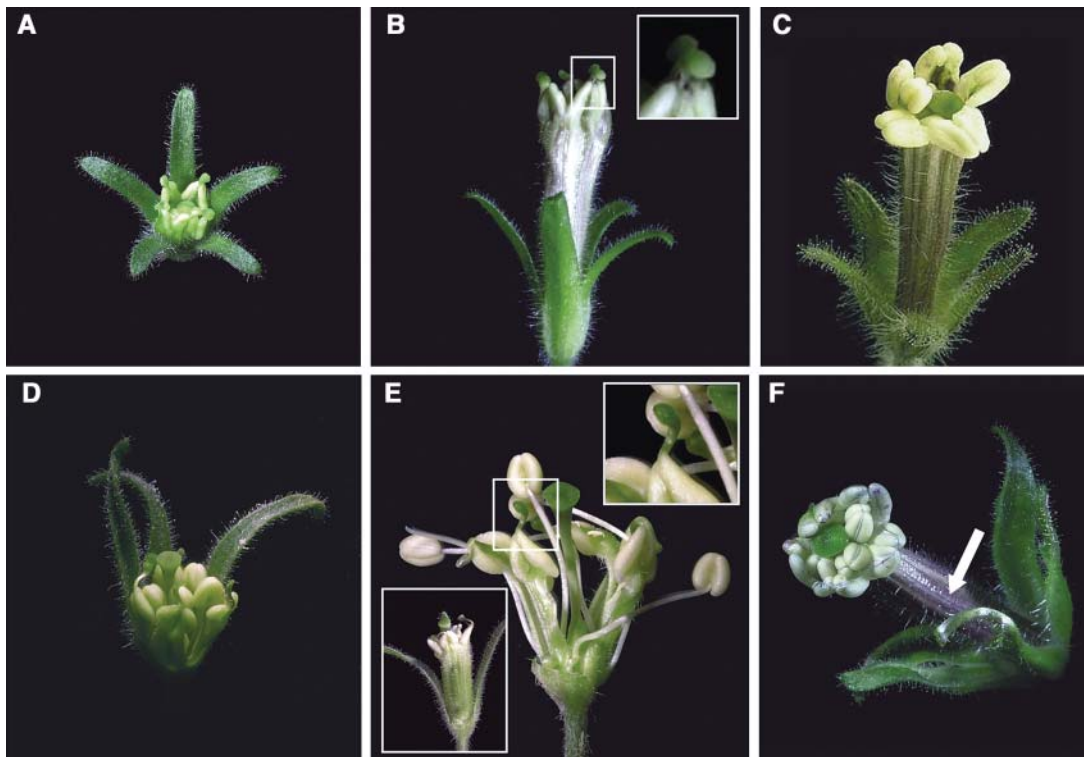

Figure 3. Flower Phenotypes of *bl* Single and *phglo1 bl*, *phdef bl*, and *phglo2 bl* Double Mutants.

(A) and **(B)** Young and full-grown *phglo1 bl* flowers, respectively, displaying second-whorl organs consisting of a tube carrying antheroid structures with stigmas on top (inset).

(C) Full-grown *bl* flower with second-whorl organs terminating with antheroid structures.

(D) and **(E)** Flowers of young and full-grown *phdef bl* double mutants, respectively, showing the presence of second-whorl organs consisting of antheroid structures with short style–stigma structures on top (top inset). Third-whorl anthers appear as wild type. Two sepals in **(D)** and all sepals in **(E)** have been removed. Bottom inset, full-grown *phdef bl* flower with a short greenish tube.

(F) *phglo2 bl* flower, phenotypically identical to *bl* single mutant flowers. The arrow indicates one of the sepal tips that is fully converted to a style–stigma structure. This aspect of the phenotype of *bl* mutant flowers is only rarely observed.

organs that are fully converted to sepals, suggesting a complete absence of B-function activity in the second whorl. Therefore, because C-function genes are ectopically expressed in the second whorl of *bl* flowers, one would expect that the second-whorl organs of *phdef bl* double mutants would entirely consist of carpelloid organs rather than the observed antheroid structures carrying small style–stigma structures on top. This phenotype suggests that *P. hybrida* contains a B-class gene, presumably a *DEF/AP3* homolog, which can complement the *phdef* mutation regarding antheroid formation in the second whorl of *phdef bl* double mutants but that is unable to complement petal development in the second whorl of *phdef* single mutants. Most likely, this postulated B-class gene represents the same gene that is responsible for the rescue of stamen development in the third whorl of *phdef* single mutants. *PhTM6*, a *P. hybrida DEF/ AP3* homolog, is the most logical candidate to represent this gene (Figure 1), although we cannot at this point formally exclude the possibility that another yet unknown candidate gene might be involved. To further investigate this, we have included the *bl* single and *phdef bl* double mutants in the expression analysis of the B-class genes described below.

RT-PCR Expression Analysis in Wild-Type and Mutant Floral Organs

To further elucidate regulatory interactions between the four *P. hybrida* B-class MADS box genes and to correlate these with the

observed phenotypes, we have monitored their expression levels in the floral whorls of the wild type and a selection of informative mutant combinations by reverse transcription (RT)–PCR.

In wild-type *P. hybrida* flowers (Figure 4A), the expression domain of the two *PI* homologs *PhGLO1* and *PhGLO2* and the eu*AP3* homolog *PhDEF* is mainly confined to the second and third whorls, as described previously (Angenent et al., 1992; van der Krol et al., 1993), and signals are slightly stronger in 0.5-cm buds compared with the later stage. Low levels of *PhDEF* expression were also detected in the first and fourth whorls, confirming earlier observations (Tsuchimoto et al., 2000), which has also been reported for *DEF* in *A. majus* (Schwarz-Sommer et al., 1992). The expression patterns of *PhGLO1*, *PhGLO2*, and *PhDEF* are thus very similar to their counterparts in Arabidopsis and *A. majus*. By contrast, the expression of *PhTM6* (a paleo*AP3*-type gene) differs drastically in this respect. Highest signals for *PhTM6* transcripts in 0.5-cm buds are detected in carpels and stamens, whereas expression levels observed in petals and sepals are much lower. In 4- to 5-cm buds, *PhTM6* levels remain high in the fourth whorl while declining in the stamens. Notably, *L. esculentum TM6* (another paleo*AP3*-type gene) transcripts also accumulate to high levels in the center of the flower (Pnueli et al., 1991).

In the various B-mutant combinations (Figure 4B), the expression patterns of *PhGLO1*, *PhGLO2*, and *PhDEF* are highly consistent with the observed phenotypes; in all fully converted
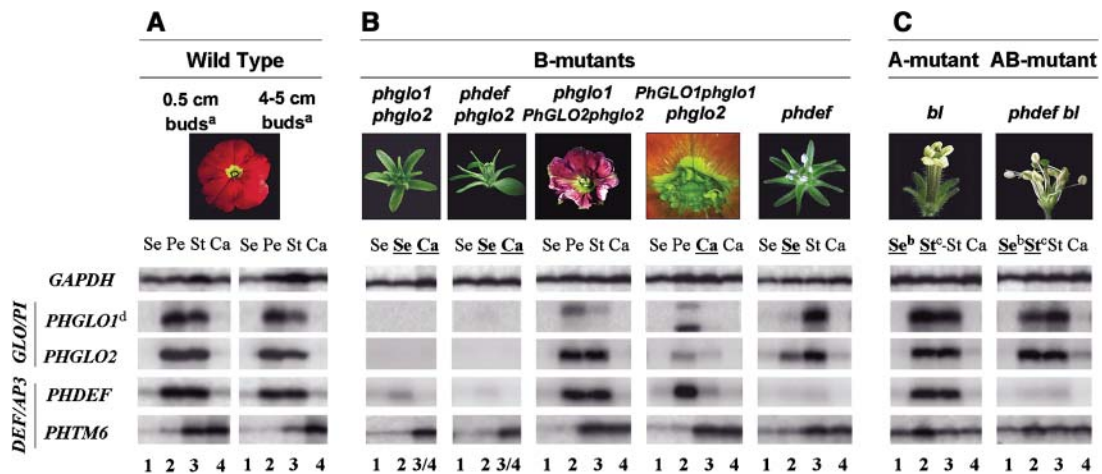

Figure 4. Expression Analysis of the Four *P. hybrida* B-Class MADS Box Genes in Floral Organs of Wild-Type and Various Mutant *P. hybrida* Flowers as Determined by RT-PCR.

(A) Expression in wild-type flowers.
(B) Expression in flowers of a selection of informative B-class mutant combinations.
(C) B-class gene expression in flowers of an A-function mutant (*bl*) and an AB-function double mutant (*phdef bl*).
Ca, carpel; Pe, petal; Se, sepal; St, stamen. Homeotically converted organs are shown in bold and underlined. Whorl numbers are indicated below the gel images. Expression of glyceraldehyde-3-phosphate dehydrogenase was monitored as a positive control. a, size indications of the flower buds reflect petal length; b, sepals harvested from *bl* and *phdef bl* flowers have been enriched for having a strong penetration of the *bl* first-whorl phenotype, consisting of sepals carrying stigmatoid tissue on the tips; c, second-whorl tissue harvested from *bl* and *phdef bl* flowers consists of antheroid structures and antheroid structures topped with style–stigma structures, respectively; d, the gene-specific primer pair designed to monitor *PhGLO1* expression flanks the insertion site of the *phglo1-2* footprint allele. This results in the amplification of a slightly larger fragment than from samples containing the wild-type allele.

organs in the different B-class mutant combinations, the expression levels of these genes are either below detection limit or significantly reduced. By contrast, the expression level of *PhTM6* in *phdef*, *phglo1 phglo2*, *phdef phglo2*, and *PhGLO1phglo1 phglo2* does not differ from the wild type, indicating that its expression at the transcriptional level is not regulated by *PhDEF*, *PhGLO1*, or *PhGLO2*.

In flowers of the A-function *bl* mutant (Figure 4C), expression patterns of *PhGLO1*, *PhGLO2*, and *PhDEF* appear as in the wild type, mainly confined to second- and third-whorl organs, as described previously (Angenent et al., 1992, Tsuchimoto et al., 1993). By contrast, *PhTM6* expression levels in a *bl* mutant background are clearly upregulated in second-whorl organs and to a lesser extent in first-whorl organs as compared with the wild type. This is quite surprising because in the original ABC model of flower development, high expression levels of B-class MADS box genes have been proposed to be confined to the second and third whorls only, independently from A- and C-function activity, as we observe for *PhGLO1*, *PhGLO2*, and *PhDEF*. In flowers of *phdef bl* double mutants, expression levels of *PhGLO1* and *PhGLO2* in the third whorl and in the second whorl are comparable to the wild type, confirming earlier observations (Tsuchimoto et al., 2000). This differs from what is observed in *phdef* flowers, where *PhGLO1* and *PhGLO2* expression levels are reduced in the second-whorl sepaloids (Figure 4B), indicating that *PhDEF* is required for the upregulation of *PhGLO1* and *PhGLO2* in the second whorl in wild-type flowers but not in the second whorl in *bl* flowers. Similar to what we observe in *bl* single mutants, *PhTM6* is mainly expressed in whorls 2, 3, and 4 and at slightly lower levels in the first whorl, indicating that the absence or presence of *PhDEF* transcripts does not influence the upregulation of *PhTM6* in the second and first whorls of *bl* flowers. Strikingly, the *PhTM6* expression pattern in wild-type, *bl*, and *phdef bl* flowers offers a very logical explanation for the unexpected second-whorl phenotype of *phdef bl* mutants (see Discussion).

In Situ Hybridization

To further analyze the expression patterns of the *P. hybrida* B-class MADS box genes during the early stages of flower development, we have monitored the spatial and temporal expression patterns of *PhTM6* and *PhGLO2* by in situ hybridization (Figure 5). Expression patterns of *PhGLO1* and *PhDEF* during early flower development have been documented previously (Angenent et al., 1995).

PhGLO2 transcripts are first detected in the very early stamen and petal primordia, where transcripts are initially uniformly distributed (Figure 5A) and remain localized in these organs during further development (Figures 5B and 5C). The *PhGLO2* expression pattern during early development is thus very similar to *PhGLO1* (Angenent et al., 1995). To illustrate *PhTM6* expression in comparison with *PhGLO2*, we have selected similar developmental stages of wild-type and *bl* flower buds. In early stage wild-type buds with emerging stamen and petal primordia (Figure 5D), highest levels of *PhTM6* expression are detected in stamen primordia and in the center of the flower bud. Signal is
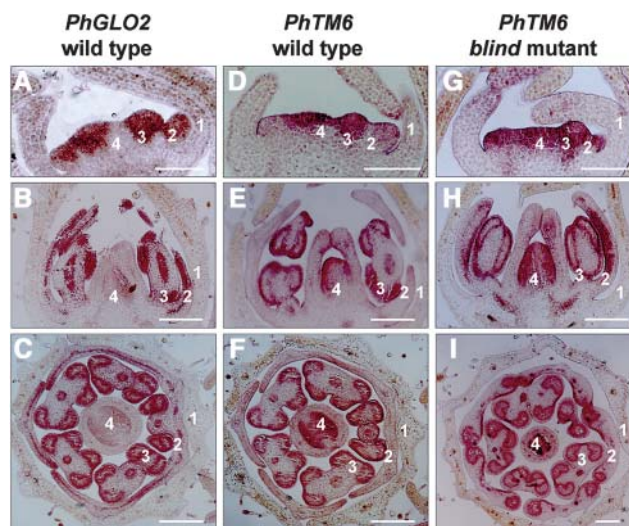

Figure 5. In Situ Localization of *PhGLO2* and *PhTM6* Transcripts in *P. hybrida* Flower Buds.

Sections were hybridized with digoxigenin-labeled antisense RNA probes of *PhGLO2* ([**A**] to [**C**]) and *PhTM6* ([**D**] to [**I**]). Cross-sections of large flower buds are shown in **(C)**, **(F)**, and **(I)**. All others are longitudinal sections. The first two columns show sections of wild-type *P. hybrida* flower buds; the last column consists of sections of *bl* mutant flower buds. First- to fourth-whorl organs are indicated by the according numbers. The red color reflects the presence of transcripts.

(A) Young wild-type flower bud with developing sepals and petals, stamen, and carpel primordia. *PhGLO2* expression is detected in petal and stamen primordi, but not in sepals and in the center of the flower.

(B) and **(C)** *PhGLO2* expression remains localized in petals and stamens during further development.

(D) Young wild-type floral bud at a comparable stage as in **(A)**. In contrast with *PhGLO2*, highest levels of *PhTM6* mRNA are present in stamen primordia and in the center of the flower, whereas low levels are detected in petal primordia.

(E) and **(F)** *PhTM6* expression during stages as in **(B)** and **(C)**. Highest expression levels are found in the developing pistil, especially in the tissue that will give rise to the placenta and ovules and in the stamens. Very low *PhTM6* levels can be observed in the developing petals.

(G) Young *bl* mutant flower bud at a similar developmental stage as in **(A)** and **(D)**. The three inner whorls show comparable *PHTM6* expression levels, in contrast with *PhTM6* expression in the wild type.

(H) *PhTM6* expression in a *bl* floral bud at a similar developmental stage as in **(B)** and **(E)**. The upregulation of *PhTM6* expression in second-whorl organs is very pronounced compared with the wild type. Note that second-whorl organs start to enlarge according to the adaxial-abaxial axis, which finally will result in the formation of a tube terminating in five antheroid structures.

(I) *bl* floral bud at a slightly later developmental stage compared with **(C)** and **(F)**, which allows capturing sections through the anthers and the well-developed second-whorl antheroid organs in the same plane. *PhTM6* mRNA accumulates in the developing ovules and placental tissue, in the third-whorl anthers, and in the second-whorl antheroid structures.

Scale bars = 100 μm in **(A)**, **(D)**, and **(G)**; 200 μm in **(B)**, **(C)**, **(E)**, **(F)**, **(H)**, and **(I)**.

also present in the emerging petal primordia but at a lower level compared with third and fourth whorls. During later stages of development (Figures 5E and 5F), expression in the petals drops further in comparison with stamens and pistil, where high expression levels are maintained. During development of the pistil, *PhTM6* expression is mainly confined to the cells that give rise to the placental tissue and ovules. In *bl* flowers, *PhTM6* expression levels and localization in third- and fourth-whorl organs are comparable to wild-type flowers throughout development (Figures 5G to 5I). By contrast, expression in the developing second-whorl organs is clearly upregulated and during later stages accumulates to levels comparable to third-whorl expression, even before the antheroid nature of the *bl* second-whorl organs becomes apparent (Figures 5G and 5H). Note that a weak signal can also be seen in the left sepal tip of the bud in Figure 5G. At a slightly later stage, the distal ends of the *bl* second-whorl organs adapt an antheroid morphology, which is clearly visible in the cross-section shown in Figure 5I. At this stage, *PhTM6* expression in the second-whorl organs is mainly localized in the developing antheroid tissues. These results are in full agreement with the RT-PCR data.

P. hybrida DEF/GLO Heterodimer Formation: Promiscuity and Monogamy

It was demonstrated previously that PHDEF is able to interact with both PHGLO1 and PHGLO2 (Immink et al., 2003), indicating that heterodimer formation between DEF/AP3 and GLO/PI proteins is conserved in *P. hybrida*. We have further investigated protein–protein interactions among the four *P. hybrida* B-class proteins using the yeast GAL4 two-hybrid system. Growth of yeast colonies on selective media was scored after 7 d of incubation at 20°C (Table 2). Interactions could be demonstrated between PHDEF and both PHGLO1 and PHGLO2, confirming previous results. In contrast with PHDEF, our data indicate that PHTM6 is only capable of interacting with PHGLO2 in yeast. However, after a prolonged incubation of 10 d, limited yeast growth could also be detected in the PHTM6/PHGLO1 combination (but not in the PHTM6/PHDEF combination and in the

Table 2. B-Class MADS Box Protein Interactions as Determined by the Yeast GAL4 Two-Hybrid System

Putative Heterodimer	−LT X-α-GAL Assay	−LTH +10 mM 3-AT	−LTHA
BD-PHDEF + AD-PHGLO1	Blue	+	+
BD-PHDEF + AD-PHGLO2	Blue	+	+
BD-PHDEF + AD-PHTM6	White	−	−
BD-PHGLO2 + AD-PHTM6	Blue	+	+
BD-PHGLO1 + AD-PHTM6	White	−	−

Yeast colonies coloring blue when grown on plates supplemented with X-α-GAL indicate interaction; white colonies indicate no interaction. + symbol indicates growth and hence interaction; − symbol indicates no growth of the yeast cells on the selective medium. All experiments were conducted at 20°C. A, Ade; H, His; L, Leu; T, Thr; 3-AT, 3-amino-1,2,4-triazole.

negative control), suggesting that PHTM6 and PHGLO1 might also be capable of interacting, although very weakly. Nevertheless, these results suggest that PHGLO2 might be the preferred interaction partner of PHTM6, although we cannot exclude the possibility that in vivo additional factors are present, which may stabilize PHTM6/PHGLO1 heterodimers.

DISCUSSION

Duplicated B-Class Genes May Diverge in Function

Whereas in both *A. majus* and Arabidopsis a single pair of genes interacts to define the developmental fate of the meristems in whorls 2 and 3, the situation in *P. hybrida* is more complicated: two *GLO/PI* as well as two *DEF/AP3* subfamily members have been identified, the latter consisting of a eu*AP3*-type (*PhDEF*) and a paleo*AP3*-type (*PhTM6*) gene. Theoretically, when both genes encoding the two partners in a DEF/GLO (or AP3/PI)-type heterodimer undergo duplication, four heterodimers can be expected: DEF1/GLO1, DEF1/GLO2, DEF2/GLO1, and DEF2/GLO2. Eventually, this redundancy might lead to the loss of one or both of the duplicated copies, or alternatively, subfunctionalization and/or neofunctionalization might lead to retention of the extra copies. According to this duplicated B-class heterodimer model and assuming that eudicot B-class MADS box proteins can only act as heterodimers consisting of a DEF/AP3 and a GLO/PI member, *def1 def2* and *glo1 glo2* double mutants should result in full homeotic conversions of both the second and the third whorls, whereas the phenotype of the remaining double mutant combinations depends on the extent to which the duplicated genes have functionally diverged.

The Largely Redundant *PhGLO1* and *PhGLO2* Genes Are Required for B-Function Activity in *P. hybrida*

To elucidate the biological role of the two *GLO/PI* homologs in *P. hybrida*, we have applied an insertion mutagenesis approach to obtain loss-of-function alleles. *phglo1* flowers display only a very local change from petal to sepal identity in the second whorl, whereas the stamen filaments and tube remain unfused. This indicates that *PhGLO1* controls the formation of the petal midvein and growth under the zone of petal and stamen initiation, which causes the corolla tube and stamen filaments to emerge as a congenitally fused structure. Interestingly, nonfusion was also observed in *phdef* flowers and in mild *PhDEF* cosuppression lines, which still developed petals (van der Krol et al., 1993), suggesting that PHDEF and PHGLO1 jointly direct this process. *phglo2* flowers on the other hand exhibit a wild-type architecture, although pollen maturation might be affected. Thus, for both *PhGLO1* and *PhGLO2* loss-of-function mutations, the drastic homeotic conversions as seen in Arabidopsis *pi* and Antirrhinum *glo* mutants were not observed. This, together with the fact that *PhGLO1* (Angenent et al., 1995) and *PhGLO2* (Figures 4 and 5) exhibit similar expression patterns in developing flowers, suggested that *PhGLO1* and *PhGLO2* act largely redundantly in petal and stamen development. This is confirmed by the phenotype of *phglo1 phglo2* flowers, which display a complete homeotic change from petals to sepals and stamens to carpels.

Moreover, this phenotype indicates a complete absence of B-function activity, implying that the two *P. hybrida DEF/AP3* homologs *PhDEF* and *PhTM6* by themselves or together do not exert B-function activity. This is in full accordance with the predictions based on a duplicated B-class heterodimer model. The function of *PhGLO1* has been analyzed previously using a cosuppression approach (Angenent et al., 1993). The transgenic lines with the most severe alterations exhibited flowers with a phenotype identical to *phglo1 phglo2* double mutants, indicating that cosuppression in these lines did not occur in a gene-specific way (cf. Vandenbussche et al., 2003b).

DEF/GLO Heterodimer Formation in Relation to Petal and Stamen Development

The results of the yeast two-hybrid analyses indicate that like in Antirrhinum and Arabidopsis, *P. hybrida* B-class MADS box proteins form heterodimers consisting of a DEF/AP3-like protein combined with a GLO/PI-like protein. Here, we integrate these data with the results obtained from the expression and mutant analyses into a model describing petal and stamen development in *P. hybrida* (Figure 6A).

Concerning the involvement of two *DEF/AP3*-like proteins in petal development, we found that in contrast with *PhDEF*, *PhTM6* is expressed at very low levels in the developing petals, indicating that *PhTM6* might not be involved in petal development. Therefore, according to the duplicated B-class heterodimer model, *phdef* mutations should result in full homeotic conversion of petals to sepals because in this whorl, the only putatively available DEF/AP3 partner, PHDEF, is mutated. This is indeed supported by the phenotype of *phdef* flowers (Figure 2K). Second, we and others (Immink et al., 2003) found that PHDEF is capable of interacting with PHGLO1 and PHGLO2, both of which are well expressed in developing petals. This indicates that PHGLO1 and PHGLO2 might exhibit functional redundancy as common interacting partners of PHDEF. This is confirmed by

the phenotype of *phglo1 phglo2* double mutants (Figure 2G). Therefore, we conclude that petal development is controlled by the largely redundant PHDEF/PHGLO1 and PHDEF/PHGLO2 heterodimers, whereas PHTM6 most likely is not involved in this process.

The expression analysis further shows that *PhTM6* is well expressed in developing stamens, as has been found for *PhDEF*, *PhGLO1*, and *PhGLO2*, indicating that all four identified B-class MADS box genes might be involved in stamen development. The phenotypes of *phglo1 phglo2* and *phdef phglo2* mutants (Figures 2G and 2P) indeed directly prove the involvement of *PhDEF*, *PhGLO1*, and *PhGLO2* in stamen development, and the two-hybrid analysis suggests that these genes act through the formation of PHDEF/PHGLO1 and PHDEF/PHGLO2 heterodimers. The two-hybrid analysis further indicated that PHTM6 interacts specifically with PHGLO2 and to a much lesser degree with PHGLO1, suggesting that the PHTM6/PHGLO2 heterodimer (and presumably not PHTM6/PHGLO1) might also be involved in stamen development. Integrating this information in the duplicated B-class heterodimer model and assuming that the capacity to form a heterodimer is a prerequisite for B-function activity, than the following predictions can be made: In *phdef phglo2* double mutants, the only available heterodimer is PHTM6/PHGLO1. However, the two-hybrid analysis revealed only a very weak interaction, if any at all, for these proteins. Therefore, in *phdef phglo2* double mutants, B-function activity should be severely reduced or completely absent. On the other hand, in *phdef phglo1* mutants, the only heterodimer theoretically available is PHTM6/PHGLO2, and the strong two-hybrid interaction between these proteins indicates that this heterodimer might be functional in vivo. The phenotypes obtained in the double mutants are in full agreement with these interpretations. In *phdef phglo2* flowers (Figure 2P), stamens are fully replaced by carpels, indicating that the PHTM6/PHGLO1 heterodimer is not formed or not sufficient to confer stamen identity. On the other hand, *phdef phglo1* flowers still develop stamens (Figure 2N), suggesting that the PHTM6/PHGLO2 heterodimer might be
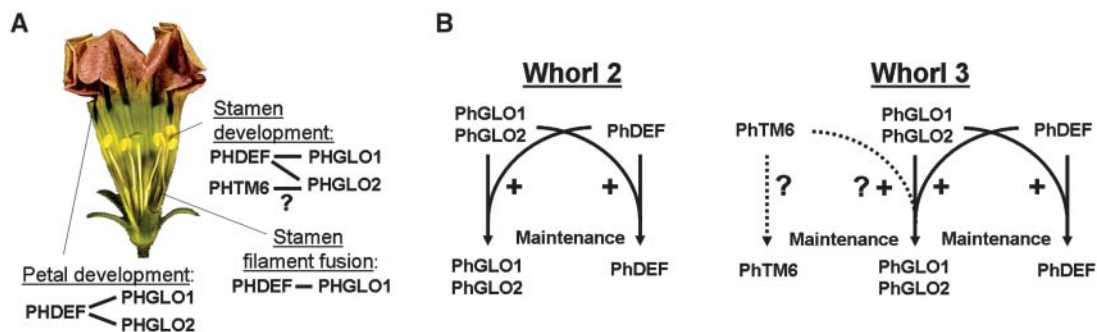

Figure 6. Summarizing Model Describing Unique and Redundant Functions of the Proposed *P. hybrida* B-Class Heterodimers and the Regulatory Interactions among These Genes Based on Mutant Analyses, Two-Hybrid Interactions, and Expression Studies.

(A) Functions of the proposed heterodimers in wild-type flowers. The two-hybrid interaction data are represented by solid lines between the involved B-class proteins.
(B) Regulatory interactions among the *P. hybrida* B-class MADS box genes.
The proposed function of the PHTM6/PHGLO2 heterodimer and the regulatory interactions involving *PhTM6* need to be confirmed.

sufficient to induce stamen development. The partner preference of PHTM6 toward PHGLO2 as suggested by the yeast two-hybrid analysis is thus strongly supported by the phenotypes of these mutants.

Functional Divergence within the *DEF/AP3* Lineage during Evolution: Defining Functions for *PhDEF* and *PhTM6*

Within the *DEF/AP3* subfamily, a major duplication event was identified that coincides with the base of the higher eudicot radiation, resulting in two types of DEF/AP3-like proteins, which can easily be distinguished on the basis of their completely divergent paleo*AP3* and eu*AP3* C-terminal motifs (Kramer et al., 1998). Whereas eu*AP3* genes appear to control stamen and petal identity in higher eudicot species, paleo*AP3* genes until now have only been characterized in the monocot species maize (*Zea mays*) and rice (*Oryza sativa*). Both the *SILKY1* and *OsMADS16* (*SPW1*) genes (Figure 1) have been shown to control stamen and lodicule identity (Ambrose et al., 2000; Nagasawa et al., 2003). Recently, data involving C-terminal motif swapping experiments were published indicating that paleo*AP3* and eu*AP3* motifs within the eudicot lineage encode divergent functions (Lamb and Irish, 2003); a chimeric construct containing the Arabidopsis *AP3* gene, of which the C-terminal eu*AP3* motif was replaced by a paleo*AP3* motif, was able to partially rescue stamen development in an *ap3-3* mutant background, whereas second-whorl organs remained fully sepaloid. These results indicate that the C-terminal motif of paleo*AP3* proteins promotes stamen but not petal development in higher eudicots, supporting the hypothesis that eu*AP3* genes may have obtained a novel function, leading to the development of petals.

In *P. hybrida*, all currently available data fit this hypothesis. Null mutations in the *P. hybrida* eu*AP3*-like *PhDEF* gene cause homeotic alterations in the second whorl of the flower, whereas stamen development remains largely unaffected. Further, we and others (Tsuchimoto et al., 2000) have shown that *phdef bl* flowers develop antheroid organs in the second whorl, although the full conversion of petals to sepals in *phdef* flowers implies a complete absence of B-function activity in the second whorl in a *phdef* genetic background. According to the duplicated B-class heterodimer model, this suggests that the paleo*AP3*-like *PhTM6* is able to complement the *phdef* mutation in stamen development but not in petal development. The expression pattern of *PhTM6* in wild-type, *phdef*, *bl*, and *phdef bl* flowers indeed fully supports this hypothesis: In wild-type and *phdef* flowers, *PhTM6* is highly expressed in the developing stamens, but only at low levels in the second-whorl petals. On the other hand, in the second-whorl antheroid organs of *bl* and *phdef bl* flowers, *PhTM6* expression is strongly upregulated to levels comparable to third-whorl expression levels in wild-type developing stamens. Finally, the phenotype of *phglo1 phglo2* and *phdef phglo2* flowers together with the two-hybrid analysis indicate that PHTM6 requires PHGLO2 for B-function activity, suggesting that PHTM6 B-function activity can be abolished through mutagenesis of its interaction partner, PHGLO2. Recently, we obtained *phdef phglo2 bl* triple mutants, and in contrast with *phdef bl* flowers, these flowers do exhibit a full homeotic conversion to carpels in the second whorl (M.

Vandenbussche, S. Royaert, and T. Gerats, unpublished data). Although a full functional analysis of *PhTM6* will be required to unequivocally prove it, this suggests that *PhTM6* is responsible for the rescue of stamen development in the third whorl of *phdef* flowers and in the second and third whorls of *phdef bl* flowers. *PhTM6* is thus a very likely candidate to represent gene *X* as postulated by Tsuchimoto et al. (2000). It may be noted that *PhTM6*, by sequence a B-function gene, behaves as a C-function gene both in respect to its wild-type expression pattern as well as its changed pattern in an A-function mutant background.

Regulatory Interactions

In both Arabidopsis and *A. majus*, it has been shown that the expression of either one of the B-function genes is initiated independently but that the maintenance of high levels of AP3 and PI depends upon the presence of the heterodimeric protein complex itself. In *A. majus*, this interdependence occurs in both whorls 2 and 3, where *DEF* and *GLO* gene products are required to regulate each others' expression positively at the level of transcription. In Arabidopsis, such an interdependent relationship exists on the transcriptional level between *AP3* and *PI* in whorl 3, but *AP3* continues to be transcribed in the second-whorl sepals in a *PI* mutant background. AP3 protein is however not detected in second-whorl organs of *pi* mutants (Jack et al., 1994). The results from our RT-PCR analysis (Figure 4) indicate that for *PhDEF* on the one hand and for *PhGLO1* or *PhGLO2* on the other hand, a similar interdependent relation at the transcriptional level exists, as has been found in Antirrhinum. In *phglo1 phglo2* flowers, *PhDEF* expression is strongly reduced in whorls 2 and 3, indicating that *PhDEF* requires the presence of at least one of the two *GLO/PI* homologs to maintain its own expression. Similarly, in the second whorl of *phdef* mutants, the expression levels of both *PhGLO1* and *PhGLO2* are reduced, suggesting that these genes require *PhDEF* to maintain high levels of expression in the second whorl (Van der Krol et al., 1993). In the third whorl of *phdef* flowers, *PhGLO1* and *PhGLO2* are still expressed at high levels, indicating that another gene, most likely *PhTM6*, acts redundantly with *PhDEF* to maintain expression of the *P. hybrida GLO* genes (see below). Nevertheless, in *phdef phglo2* flowers, expression levels of *phdef*, *PhGLO1*, and *phglo2* are severely downregulated in both the second and third whorls. Other evidence that *PhDEF* affects the expression of *PhGLO1* and *PhGLO2* came from transgenic lines overexpressing *PhDEF* (Halfter et al., 1994). In these lines, sepals are converted to petals, and *PhGLO1* and *PhGLO2* are ectopically expressed in these converted tissues.

By contrast, the expression pattern of *PhTM6* remained virtually unchanged in all tested B-function mutants, indicating that maintenance of *PhTM6* expression at the transcriptional level does not depend on the activity of *PhDEF*, *PhGLO1*, and *PhGLO2*. A schematic representation of all of these regulatory interactions in wild-type *P. hybrida* flowers is shown in Figure 6B.

Further, we found that *PhTM6* is upregulated in the second whorl of *bl* flowers (and to a lesser degree in the first whorl), indicating that *PhTM6* expression either is repressed by the *BL* gene product or, alternatively, that *PhTM6* requires C-function activity to maintain high expression levels. The latter hypothesis

is consistent with the idea that B- and C/D-function genes originally might have been more tightly associated with each other in reproductive organ development, before specialized sterile perianth organs appeared during flower evolution (Theissen et al., 2000, and references therein). Unfortunately, we cannot yet verify the hypothesis that *PhTM6* requires C-function activity because C-function mutants are not yet available in *P. hybrida*. Finally, our data suggest that both *PhGLO1* and *PhGLO2* expression in whorl 3 of *phdef* mutants and in whorls 2 and 3 of *phdef bl* flowers is possibly maintained by *PhTM6*, despite the fact that at least in in vitro experiments, *PhTM6* appears to interact only with *PhGLO2* on the protein level. A plausible explanation for this would be that although PHTM6 is not capable of heterodimerizing with PHGLO1, the PHTM6/PHGLO2 heterodimer might be capable of activating *PhGLO1* expression.

B-Class Gene Dosage Modulates the Developmental Fate of Second- and Third-Whorl Meristems in a Quantitative and Qualitative Manner

Normally, B-class gene dosage is not directly associated with phenotypic changes in flower morphology. Like the known B-class mutant alleles from Arabidopsis and Antirrhinum, all available *phglo1*, *phglo2*, and *phdef* mutations are fully recessive, implying that a reduction of 50% in gene dosage because of the presence of a mutant allele in a heterozygous state does not induce any phenotypic effect. However, when a function that is normally encoded by one gene is duplicated, gene dosage can be further reduced to a level of 25% in plants homozygous mutant for gene copy A and heterozygous for gene copy B. This readily explains our observation of gene dosage effects in specific progeny classes, as, for example, in the second whorl of *PhDEFphdef phglo1* flowers and in the second and third whorls of *phglo1 PhGLO2phglo2* flowers (Figures 2I, 2J, 2O, and 2Q). Further, in *PhGLO1phglo1 phglo2* flowers, second-whorl organs fully retain their petal identity, whereas stamens are replaced by carpelloid structures (Figures 2H, 2L, 2M, and 2Q). This indicates that the sensitivity of petal and stamen development toward a reduction in B-class gene dosage differs and that the third whorl apparently requires a higher dose of B-function activity to maintain normal identity. Remarkably, a similar phenomenon was observed in Antirrhinum in heterozygous plants carrying a *def* null allele in combination with the temperature sensitive *def-101* allele (Schwarz-Sommer et al., 1992; Zachgo et al., 1995). Gene dosage effects have also been described for specific *sepallata* mutant combinations (Favaro et al., 2003).

Evolution of *P. hybrida* B-Function Regulation Compared with Antirrhinum and Arabidopsis

The data presented here demonstrate that gene duplications in the *DEF/AP3* and *GLO/PI* lineages in *P. hybrida* have led to a functional diversification of their respective members, which is reflected by partner specificity and whorl-specific functions among these proteins. Nevertheless, when the individual actions of *PhDEF*, *PhGLO1*, and *PhGLO2* are considered together, they appear basically to function in a similar way as *DEF/GLO* in

Antirrhinum and *AP3/PI* in Arabidopsis. Analyzed in more detail, the *P. hybrida* B-class loss-of-function phenotypes and the regulatory network among these genes resemble more the situation in Antirrhinum than in Arabidopsis, which is logical given the taxonomic distribution of the three species. In addition, we identified a novel function fulfilled by a B-class heterodimer: PHDEF/PHGLO1 seems to be controlling the fusion of the stamen filaments with the petal tube. In Antirrhinum and Arabidopsis, this function apparently is not present because in these flowers, wild-type stamens emerge as freestanding structures. This might be an example of a subtle difference in function that accounts for species-specific differences in floral architecture.

In contrast with what we found for *PhDEF*, all current data indicate that the function and mode of action of the paleo*AP3*-type PHTM6 differs significantly from the known eu*AP3*-type DEF/AP3-like proteins; *PhTM6* is mainly expressed in the third and fourth whorls, its maintenance of expression does not require functional GLO/PI-like proteins, its expression pattern is altered in an A-function mutant background, and most likely *PhTM6* is not involved in petal development. The latter is consistent with the hypothesis that the evolutionary origin of the higher eudicot petal structure coincided with the appearance of eu*AP3*-type MADS box genes (Kramer et al., 1998; Lamb and Irish, 2003; Vandenbussche et al., 2003a). Future research focused on a functional analysis of *PhTM6* may shed new light on the recruitment of B-class MADS box genes in petal and stamen development during evolution.

METHODS

Phylogenetic Analysis

The neighbor-joining tree shown in Figure 1 was obtained according to the methodology described previously (Vandenbussche et al., 2003a).

Plant Material and Genotyping

For the crosses described in this article, we have used a *phglo1-2* line in which the *dTph8* transposon has excised, leaving behind a 5-bp footprint, which introduces a stop codon at amino acid position 143 of the *PhGLO1* coding sequence. This *phglo1-2*–derived footprint allele induces an identical phenotype as the *phglo1-1* and the original *phglo1-2* alleles. From the *phglo2* alleles (Table 1), we have selected *phglo2-3* because in this line, the first exon encoding the DNA binding MADS domain is disrupted by the transposon insertion, most likely resulting in a null mutation. Homozygous *phglo1-2*, *phglo2-3*, and *phdef-1* mutants were crossed with each other and to the *bl* mutant (Vallade et al., 1987), and the resulting F1 plants were self-fertilized to obtain F2 progenies. All the different phenotypic classes described segregated in agreement with the expected Mendelian ratios, and similar results were obtained when we analyzed additional F2 progenies obtained from different F1 individuals. Genotyping of the *phglo1-2* and *phglo2-3* insertion alleles was done by PCR using gene-specific forward (fw) and reverse (rv) primer pairs flanking the insertion sites (*PhGLO1*-fw, 5′-CTTGAAGGGTGAAGATAT-CACATC-3′; *PhGLO1*-rv, 5′-TTCCTCATCATCCTCAGAACCTC-3′; *PhGLO2*-fw, 5′-GAGAAGTGAGATATTAGGTATGG-3′; and *PhGLO2*-rv, 5′-GCTACAATATTCATGCATCTTGCCAGA-3′) (data not shown). Genotypes for *phdef* and *bl* mutant alleles were scored on a phenotypic basis and, in specific cases, confirmed by backcrossing with *phdef* and *bl* homozygous mutants, respectively.

Electron Microscopy

Samples for cryo-scanning electron microscopy were first frozen in slush, prepared in an Oxford Alto 2500 cryo-system (Catan, Oxford, UK), and then analyzed in a JEOL JSM-6330F field emission electron scanning microscope (JEOL, Tokyo, Japan).

RT-PCR Analysis

Total RNA from different tissues was isolated using Trizol reagent (Life Technologies, Cleveland, OH) according to the instructions of the manufacturer. First-strand cDNA synthesis was done by combining 2 μg of total RNA diluted in 20 μL with 1 μL of oligo(dT)$_{25}$ primers (700 ng/ μL), 4 μL of water, 8 μL of first-strand buffer, 4 μL of 0.1 M DTT, 2 μL of 10 mM deoxynucleotide triphosphate, and 1 μL of Superscript II RT (200 units/μL; Gibco BRL, Cleveland, OH) in a total volume of 40 μL. After incubation for 2 h at 42°C, the mixture was diluted 10 times. Five microliters of this dilution was used as a template for PCR amplification. PCR products were visualized by radiolabeling one primer of each gene-specific primer pair and analyzed by PAGE as described previously (Vandenbussche et al., 2003b). Integrity of the RNA samples and cDNA synthesis was monitored by measuring the expression level of glyceraldehyde-3-phosphate dehydrogenase as a positive control (25 PCR cycles). Signals for the B-class MADS box genes as presented here were obtained after 33 PCR cycles. Expression in the wild type was analyzed at two developmental stages (in 0.5-cm and 4- to 5-cm buds); for the mutant samples, these two stages were pooled. All reactions have been done in duplicate starting from independent RNA samples, and all results were in good agreement (data not shown). Some of the expression patterns shown here have been analyzed previously by RNA gel blot analysis; we have obtained comparable results in all cases (Angenent et al., 1992, 1995; van der Krol et al., 1993; Tsuchimoto et al., 2000).

In Situ Hybridization

3′ gene-specific fragments of *PhGLO2* and *PhTM6* were generated by PCR using gene-specific primer pairs and subsequently cloned in pGEM-T (Promega, Madison, WI), containing T7 and SP6 transcription sites. Probe synthesis and in situ hybridizations were performed as described previously (Caňas et al., 1994). Images were recorded with an AxioCam digital camera (Zeiss, Jena, Germany).

Two-Hybrid Analysis

The pBD-GAL4 bait and pAD-GAL4 prey vectors containing *PhDEF*, *PhGLO1*, or *PhGLO2* were provided by Richard Immink and described previously (Ferrario et al., 2003). A full-length cDNA copy of *PhTM6* was generated by PCR and cloned into the pAD-GAL4 vector. The GAL4 yeast two-hybrid analyses were performed as described previously (Immink et al., 2003), using the yeast strain PJ69-4a (James et al., 1996). Selection for interaction was performed on selective medium lacking His supplemented with 10 mM 3-AT (3-amino-1,2,4-triazole; Sigma, St. Louis, MO) and confirmed on selective medium lacking His and Ade and on medium supplemented with X-α-Gal (CLONTECH, Palo Alto, CA). Growth of yeast on selective media was scored after 7 d of incubation at 20°C, whereas blue staining was scored after an overnight incubation at 20°C.

Sequence Deposition

The genomic structure of *PhGLO1* (AY532265) and *PhTM6* (AY532264) was determined by sequencing PCR-generated fragments amplified from genomic DNA, covering the full coding sequence of these genes.

REFERENCES

Ambrose, B.A., Lerner, D.R., Ciceri, P., Padilla, C.M., Yanofsky, M.F., and Schmidt, R.J. (2000). Molecular and genetic analyses of the silky1 gene reveal conservation in floral organ specification between eudicots and monocots. Mol. Cell **5,** 569–579.

Angenent, G.C., Busscher, M., Franken, J., Dons, H.J., and van Tunen, A.J. (1995). Functional interaction between the homeotic genes fbp1 and pMADS1 during petunia floral organogenesis. Plant Cell **7,** 507–516.

Angenent, G.C., Busscher, M., Franken, J., Mol, J.N., and van Tunen, A.J. (1992). Differential expression of two MADS box genes in wild-type and mutant petunia flowers. Plant Cell **4,** 983–993.

Angenent, G.C., Franken, J., Busscher, M., Colombo, L., and van Tunen, A.J. (1993). Petal and stamen formation in petunia is regulated by the homeotic gene fbp1. Plant J. **4,** 101–112.

Becker, A., Kaufmann, K., Freialdenhoven, A., Vincent, C., Li, M.A., Saedler, H., and Theissen, G. (2002). A novel MADS-box gene subfamily with a sister-group relationship to class B floral homeotic genes. Mol. Genet. Genomics **266,** 942–950.

Becker, A., Winter, K.U., Meyer, B., Saedler, H., and Theissen, G. (2000). MADS-box gene diversity in seed plants 300 million years ago. Mol. Biol. Evol. **17,** 1425–1434.

Bowman, J.L., Smyth, D.R., and Meyerowitz, E.M. (1989). Genes directing flower development in Arabidopsis. Plant Cell **1,** 37–52.

Caňas, L.A., Busscher, M., Angenent, G.C., Beltran, J., and van Tunen, A.J. (1994). Nuclear localization of the petunia MADS-box protein FBP1. Plant J. **6,** 597–604.

Coen, E.S., and Meyerowitz, E.M. (1991). The war of the whorls: Genetic interactions controlling flower development. Nature **353,** 31–37.

de Vlaming, P., Cornu, A., Farcy, E., Gerats, A.G.M., Wiering, H., and Wijsman, H.J.W. (1984). Petunia hybrida: A short description of the action of 91 genes, their origin and their map locations. Plant Mol. Biol. Rep. **2,** 21–42.

Favaro, R., Pinyopich, A., Battaglia, R., Kooiker, M., Borghi, L., Ditta, G., Yanofsky, M.F., Kater, M.M., and Colombo, L. (2003). MADS box protein complexes control carpel and ovule development in Arabidopsis. Plant Cell **15,** 2603–2611.

Ferrario, S., Immink, R.G., Shchennikova, A., Busscher-Lange, J., and Angenent, G.C. (2003). The MADS box gene FBP2 is required for SEPALLATA function in petunia. Plant Cell **15,** 914–925.

Goto, K., and Meyerowitz, E.M. (1994). Function and regulation of the Arabidopsis floral homeotic gene PISTILLATA. Genes Dev. **8,** 1548– 1560.

Halfter, U., Ali, N., Stockhaus, J., Ren, L., and Chua, N.H. (1994). Ectopic expression of a single homeotic gene, the Petunia gene green

petal, is sufficient to convert sepals to petaloid organs. EMBO J. **13,** 1443–1449.

Immink, R.G., Ferrario, S., Busscher-Lange, J., Kooiker, M., Busscher, M., and Angenent, G.C. (2003). Analysis of the petunia MADS-box transcription factor family. Mol. Genet. Genomics **268,** 598–606.

Jack, T., Fox, G.L., and Meyerowitz, E.M. (1994). Arabidopsis homeotic gene APETALA3 ectopic expression: Transcriptional and posttranscriptional regulation determine floral organ identity. Cell **76,** 703–716.

James, P., Halladay, J., and Craig, E.A. (1996). Genomic libraries and a host strain designed for highly efficient two-hybrid selection in yeast. Genetics **144,** 1425–1436.

Kater, M.M., Colombo, L., Franken, J., Busscher, M., Masiero, S., Van Lookeren Campagne, M.M., and Angenent, G.C. (1998). Multiple AGAMOUS homologs from cucumber and petunia differ in their ability to induce reproductive organ fate. Plant Cell **10,** 171–182.

Kramer, E.M., Di Stilio, V.S., and Schluter, P.M. (2003). Complex patterns of gene duplication in the *APETALA3* and *PISTILLATA* lineages of the Ranunculaceae. Int. J. Plant Sci. **164,** 1–11.

Kramer, E.M., Dorit, R.L., and Irish, V.F. (1998). Molecular evolution of genes controlling petal and stamen development: Duplication and divergence within the APETALA3 and PISTILLATA MADS-box gene lineages. Genetics **149,** 765–783.

Kramer, E.M., and Irish, V.F. (1999). Evolution of genetic mechanisms controlling petal development. Nature **399,** 144–148.

Kramer, E.M., and Irish, V.F. (2000). Evolution of the petal and stamen developmental programs: Evidence from comparative studies of the lower eudicots and basal angiosperms. Int. J. Plant Sci. **16,** 29–30.

Krizek, B.A., and Meyerowitz, E.M. (1996). The Arabidopsis homeotic genes APETALA3 and PISTILLATA are sufficient to provide the B class organ identity function. Development **122,** 11–22.

Lamb, R.S., and Irish, V.F. (2003). Functional divergence within the APETALA3/PISTILLATA floral homeotic gene lineages. Proc. Natl. Acad. Sci. USA **100,** 6558–6563.

McGonigle, B., Bouhidel, K., and Irish, V.F. (1996). Nuclear localization of the Arabidopsis APETALA3 and PISTILLATA homeotic gene products depends on their simultaneous expression. Genes Dev. **10,** 1812–1821.

Nagasawa, N., Miyoshi, M., Sano, Y., Satoh, H., Hirano, H., Sakai, H., and Nagato, Y. (2003). SUPERWOMAN1 and DROOPING LEAF genes control floral organ identity in rice. Development **130,** 705–718.

Pnueli, L., Abu-Abeid, M., Zamir, D., Nacken, W., Schwarz-Sommer, Z., and Lifschitz, E. (1991). The MADS box gene family in tomato: Temporal expression during floral development, conserved secondary structures and homology with homeotic genes from Antirrhinum and Arabidopsis. Plant J. **1,** 255–266.

Purugganan, M.D., Rounsley, S.D., Schmidt, R.J., and Yanofsky, M.F. (1995). Molecular evolution of flower development: Diversification of the plant MADS-box regulatory gene family. Genetics **140,** 345–356.

Riechmann, J.L., Krizek, B.A., and Meyerowitz, E.M. (1996). Dimerization specificity of Arabidopsis MADS domain homeotic proteins APETALA1, APETALA3, PISTILLATA, and AGAMOUS. Proc. Natl. Acad. Sci. USA **93,** 4793–4798.

Schwarz-Sommer, Z., Hue, I., Huijser, P., Flor, P.J., Hansen, R., Tetens, F., Lonnig, W.E., Saedler, H., and Sommer, H. (1992).

Characterization of the Antirrhinum floral homeotic MADS-box gene deficiens: Evidence for DNA binding and autoregulation of its persistent expression throughout flower development. EMBO J. **11,** 251–263.

Sommer, H., Beltran, J.P., Huijser, P., Pape, H., Lonnig, W.E., Saedler, H., and Schwarz-Sommer, Z. (1990). Deficiens, a homeotic gene involved in the control of flower morphogenesis in Antirrhinum majus: The protein shows homology to transcription factors. EMBO J. **9,** 605–613.

Theissen, G., Becker, A., Di Rosa, A., Kanno, A., Kim, J.T., Munster, T., Winter, K.U., and Saedler, H. (2000). A short history of MADS-box genes in plants. Plant Mol. Biol. **42,** 115–149.

Theissen, G., Kim, J.T., and Saedler, H. (1996). Classification and phylogeny of the MADS-box multigene family suggest defined roles of MADS-box gene subfamilies in the morphological evolution of eukaryotes. J. Mol. Evol. **43,** 484–516.

Trobner, W., Ramirez, L., Motte, P., Hue, I., Huijser, P., Lonnig, W.E., Saedler, H., Sommer, H., and Schwarz-Sommer, Z. (1992). GLOBOSA: A homeotic gene which interacts with DEFICIENS in the control of Antirrhinum floral organogenesis. EMBO J. **11,** 4693–4704.

Tsuchimoto, S., Mayama, T., van der Krol, A., and Ohtsubo, E. (2000). The whorl-specific action of a petunia class B floral homeotic gene. Genes Cells **5,** 89–99.

Tsuchimoto, S., van der Krol, A.R., and Chua, N.H. (1993). Ectopic expression of pMADS3 in transgenic petunia phenocopies the petunia blind mutant. Plant Cell **5,** 843–853.

Vallade, J., Maizonnier, D., and Cornu, A. (1987). La morphogenese florale chez le petunia I. Analyze d'un mutant a corolle staminee. Can. J. Bot. **65,** 761–764.

Van den Broeck, D., Maes, T., Sauer, M., Zethof, J., De Keukeleire, P., D'Hauw, M., Van Montagu, M., and Gerats, T. (1998). Transposon display identifies individual transposable elements in high copy number lines. Plant J. **13,** 121–129.

van der Krol, A.R., Brunelle, A., Tsuchimoto, S., and Chua, N.H. (1993). Functional analysis of petunia floral homeotic MADS box gene pMADS1. Genes Dev. **7,** 1214–1228.

Vandenbussche, M., Theissen, G., Van de Peer, Y., and Gerats, T. (2003a). Structural diversification and neo-functionalization during floral MADS-box gene evolution by C-terminal frameshift mutations. Nucleic Acids Res. **31,** 4401–4409.

Vandenbussche, M., Zethof, J., Souer, E., Koes, R., Tornielli, G.B., Pezzotti, M., Ferrario, S., Angenent, G.C., and Gerats, T. (2003b). Toward the analysis of the petunia MADS box gene family by reverse and forward transposon insertion mutagenesis approaches: B, C, and D floral organ identity functions require *SEPALLATA*-like MADS box genes in petunia. Plant Cell **15,** 2680–2693.

Yang, Y., Fanning, L., and Jack, T. (2003a). The K domain mediates heterodimerization of the *Arabidopsis* floral organ identity genes, APETALA3 and PISTILLATA. Plant J. **33,** 47–59.

Yang, Y., Xiang, H., and Jack, T. (2003b). *pistillata-5*, an *Arabidopsis* B class mutant with strong defects in petal but not in stamen development. Plant J. **33,** 177–188.

Zachgo, S., Silva Ede, A., Motte, P., Trobner, W., Saedler, H., and Schwarz-Sommer, Z. (1995). Functional analysis of the Antirrhinum floral homeotic DEFICIENS gene in vivo and in vitro by using a temperature-sensitive mutant. Development **121,** 2861–2875.